# Inelastic electron scattering to negative parity states of $^{28}$Si

S. Yen, R. J. Sobie, T. E. Drake, and H. Zarek
*Department of Physics, University of Toronto, Toronto, Ontario, Canada M5S 1A7*

C. F. Williamson, S. Kowalski, and C. P. Sargent
*Bates Linear Accelerator and Department of Physics, Massachusetts Institute of Technology, Cambridge, Massachusetts 02139*

(Received 1 December 1982)

Negative-parity states of $^{28}$Si are studied by high-resolution inelastic electron scattering. The form factors of the $1^-$ (8.904), $5^-$ (9.702), $1^-$, $2^-$ (9.929), $3_2^-$ (10.180), and $4^-$ $T=1$ (12.664) states are determined for the first time, for momentum transfers between 0.9 and 2.4 fm$^{-1}$. The $3_1^-$ (6.879) state is studied by subtracting off the theoretical contribution of the nearby $4^+$ (6.889) state. An upper limit for the $5^-$ $T=1$ (13.248) is established. The $3^-$ $T=0/6^-$ $T=0$ complex (11.58) remains unresolved. We present evidence for oblate-prolate deformation changes in the $3^-$ $T=0$ states. The experimental data are compared with predictions of the open-shell random phase approximation of Rowe and Wong. In $^{28}$Si, the open-shell random phase approximation is demonstrated to be extremely sensitive to the ground state wave function used, and other possible limitations of the open-shell random phase approximation are discussed.

[NUCLEAR REACTIONS $^{28}$Si $(e,e')$, $E=96$–$279$ MeV, $\theta=90°$, 160°, negative parity states; measured $d\sigma/d\Omega$ $(E,\theta)$; deduced electromagnetic form factors, Tassie model parameters, $B(\lambda)$ values. Open-shell random phase approximation calculations.]

## I. INTRODUCTION

Historically, one-particle-one-hole excitations were proposed by Wilkinson[1] to explain the $E1$ photoresonance which dominates the photon absorption cross sections of even-even nuclei; however, this explanation yielded an excitation energy which was too low and a width which was too broad. Elliot and Flowers[2] showed that, by including the residual particle-hole interaction, the strength is concentrated in only a few states, resulting in a reduction of the overall width of $E1$ strength in $^{16}$O, and an increase in the excitation energy to the correct value. Gillet *et al.*[3] extended this particle-hole model of nuclear excitation to include backward-going amplitudes due to ground-state correlations. This was done via the random phase approximation (RPA), and the RPA correlations in $^{16}$O, $^{40}$Ca, and $^{208}$Pb were found to increase the collectivity of the low-lying negative parity states. Rowe and Wong then used an equations-of-motion formalism to extend the RPA to open-shell nuclei.[4] The success of this open shell RPA (OSRPA) was first demonstrated for the negative parity states of $^{12}$C.[5]

More recently, the importance of the role of single-particle properties in collective excitations of the nucleus has been further emphasized in the work of Blaizot and Gogny.[6] These workers have performed large-basis, Hartree-Fock calculations of the ground state properties of closed-shell nuclei, using a phenomenological effective interaction chosen to reproduce the bulk properties of nuclear matter: the saturation binding energy per nucleon, the Fermi momentum, and the compressibility. The same interaction in a Hartree-Fock (HF) calculation reproduces the binding energies and charge radii of the finite nuclei $^{16}$O, $^{40}$Ca, $^{90}$Zr, and $^{208}$Pb, and yields ground state wave functions as well. This HF ground state, operated on by RPA operators with the *same* interaction as that used to calculate the ground state, yields the collective negative-parity states in these nuclei. This totally self-consistent approach leads to unprecedented success in predicting, for example, the strength of the collective $3^-$ state in $^{208}$Pb.[7] However, this approach has not yet been extended to the open shell.

In this paper we consider the negative-parity states of the open-shell nucleus $^{28}$Si. Our inelastic scattering measurements are compared to the OSRPA calculations. This paper, and the companion paper on negative-parity states of $^{24}$Mg,[8] constitute the

 

most exhaustive comparison to date of OSRPA calculations with experimental data.

## II. EXPERIMENT

The experiments were performed with the high-resolution electron scattering facility at the MIT-Bates linear accelerator.[9] A typical spectrum of inelastically scattered electrons is shown in Fig. 1. The targets used were natural Si, originally of thickness 0.25 mm, and etched with hydrofluoric, nitric, and acetic acid to final thicknesses of 25 to 32 mg/cm$^2$. The targets were positioned in reflection for scattering angle $\theta=160°$, in transmission for $\theta=90°$. Typically, a resolution of 65–80 keV FWHM was achieved at $\theta=160°$, and 35–50 keV at $\theta=90°$, the resolution being limited by target thickness. Average beam currents were 20–40 $\mu$A at $\theta=160°$ and 8–20 $\mu$A for $\theta=90°$. Corrections were made for detector dead time.

In the plane-wave Born approximation (PWBA), for $q \gg \omega$, the differential scattering cross section for inelastic electron scattering from a target nucleus of mass $M_T$ to an isolated resonance is given by[10]

$$\frac{d\sigma}{d\Omega}=4\pi\sigma_m\eta_R\left[F_{c\lambda}^2(q)+\left[\tfrac{1}{2}+\tan^2\frac{\theta}{2}\right]F_{T\lambda}^2(q)\right],$$

where $d\sigma/d\Omega$ is the cross section with radiative correction applied,

$$\sigma_m=\left[\frac{a\cos\frac{1}{2}\theta}{2E_i\sin^2\frac{1}{2}\theta}\right]^2$$

is the Mott cross section,

$$\eta_R=[1+(2E_i/M_T)\sin^2\tfrac{1}{2}\theta]^{-1}$$

is a recoil correction factor, $E_i$ ($E_f$) are the incident (final) electron energies, $q$ is the three-momentum transfer, $\omega$ is the energy transfer, $F_{c\lambda}^2(q)$ is the Coulomb squared form factor, and $F_{T\lambda}^2(q)$ is the transverse squared form factor, which may be electric or magnetic. We further define the total form factor

$$F^2(q)=\frac{d\sigma/d\Omega}{4\pi\sigma_m\eta_R}.$$

Since the electron is accelerated by the Coulomb field of the target nucleus, the effective momentum transfer is actually greater than $q$ given above, and is approximately

$$q_{\text{eff}}=q\left[1+\tfrac{3}{2}\sqrt{3/5}\frac{Z\alpha}{1.05A^{1/3}E_i}\right].$$

For each resonance, we present a plot of $F^2(q_{\text{eff}})$ versus $q_{\text{eff}}$, and this is compared with theoretical PWBA squared form factors. In PWBA for a pure-

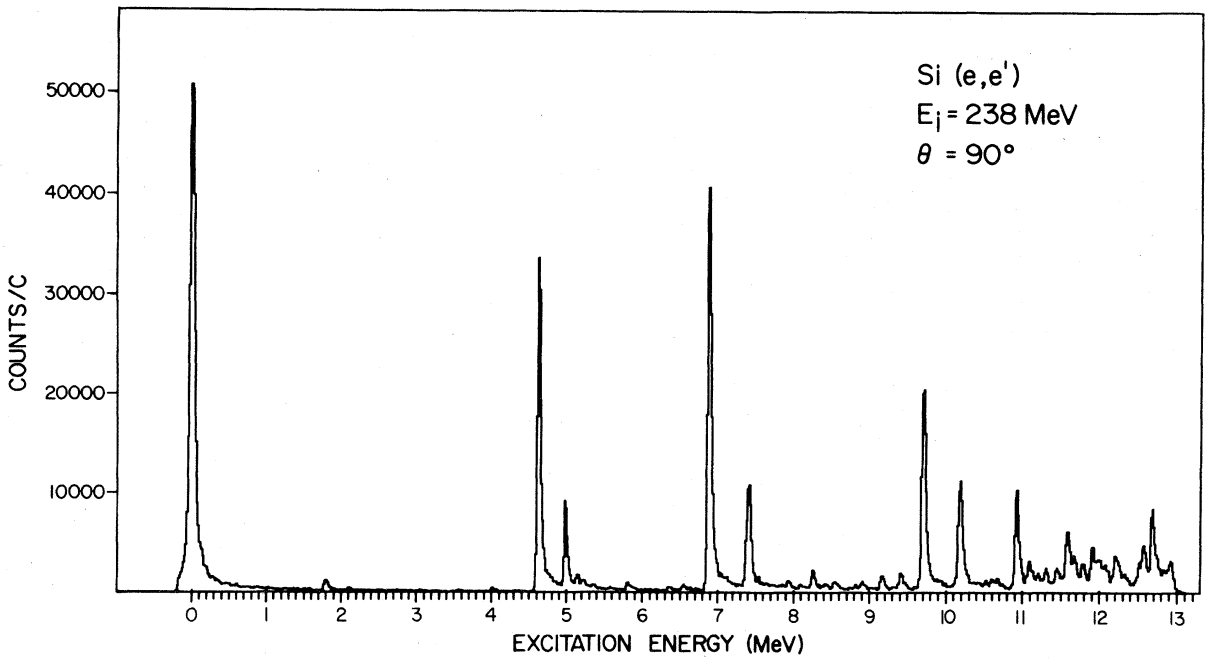


FIG. 1. Spectrum of electrons scattered from a natural Si target. The incident electron energy is 238 MeV, and the scattering angle is $\theta=90°$.

ly transverse transition, the ratio

$$R=F^2(q_{\text{eff}},\theta=160°)/F^2(q_{\text{eff}},\theta=90°)$$

is equal to 21.8, while for a pure Coulomb transition, $R=1.0$.

For natural parity excitations whose form factors are predominantly Coulomb, we shall present Tassie model[11] fits to the data. In this model, the transition charge density for a transition of multipolarity $l$ is given by

$$\rho_l(r)=r^{l-1}\frac{\partial\rho}{\partial r} ,$$

where the ground state charge density is the Fermi distribution

$$\rho=\rho_0[1+\exp(r-c)4.4/t]^{-1}$$

and $c$ and $t$ are the radius and thickness parameters, respectively.

## III. OSRPA CALCULATIONS

We have performed calculations for the negative parity states of $^{28}$Si in the open-shell random phase approximation (OSRPA) of Rowe and Wong.[4] In the OSRPA, for a $J=T=0$ ground state, an excited state $|\chi\rangle$ of multipolarity $\lambda$ is obtained from the uncorrelated ground state $|\Phi_0\rangle$ by application of an excitation operator $0^+_\lambda$:

$$|\chi\rangle=0^+_\lambda|\Phi_0\rangle ,$$

where

$$0^+_\lambda=\sum_{p>h}(n_h-n_p)^{-1/2}[Y_{ph}(\lambda)A^+_{ph}-Z_{ph}(\lambda)A_{ph}] ,$$

$p$ and $h$ are particle and hole orbitals, respectively; $n_p$ and $n_h$ are the fractional occupancies of these orbitals in the uncorrelated ground state; $A^+_{ph}$ and $A_{ph}$ are particle-hole creation and destruction operators, respectively; and $Y_{ph}$ and $Z_{ph}$ are the "forward" and "backward" amplitudes for particle-hole creation and destruction, respectively. It is convenient to define the normalized forward and backward amplitudes

$$F_{ph}=(n_h-n_p)^{1/2}\hat{T}^{-1}Y^*_{ph} ,$$
$$F_{hp}=(n_h-n_p)^{1/2}\hat{T}^{-1}(-1)^{p-h+J+T}Z^*_{ph}$$

because for any tensor one-body operator

$$W^J=\sum_T W^{JT}$$

the reduced matrix element is given by

$$\langle\chi||W^J||\Phi_0\rangle=\hat{J}_i\sum_{\mu\nu T}F_{\mu\nu}(JT)\langle\mu|||W^{JT}|||\nu\rangle ,$$

where

$$\hat{J}\equiv(2J+1)^{+1/2},\quad \hat{T}\equiv(2T+1)^{+1/2} .$$

Here

$$\langle\mu|||W^{JT}|||\nu\rangle$$

is a single-particle matrix element, $J$, $T$ refer to the spin and isospin of the final state,

$$p-h\equiv jp-jh ,$$

and $jp$, $jh$ are the angular momenta of the particle and hole orbitals. Thus all the nuclear structure information is contained in the amplitudes $F_{\mu\nu}$. In particular, if $W$ is the electromagnetic operator, then

$$|\langle\chi||W^J||\Phi_0\rangle^2$$

is, apart from a numerical factor, the squared form factor for the state $|\chi\rangle$.

Note that for a pure particle-hole excitation from a completely filled orbital $h$ to a completely empty orbital $p$, $Y_{ph}=1$ but $F_{ph}=1$ for a $T=0$ final state and $1/\sqrt{3}$ for a $T=1$ final state. All theoretical form factors presented in this paper are evaluated in the plane wave Born approximation (PWBA).

In the calculations described in this paper, three different uncorrelated ground states for $^{28}$Si are employed. The first, designated "KUO," is a shell-model ground state computed using the Oak Ridge-Rochester shell model code[12] and renormalized Kuo matrix elements[13] derived from the Hamada-Johnston potential; the model space is the full $sd$ shell. The second, designated "OBL," is a projected Hartree-Fock (PHF) oblate $0^+$ ground state computed by Castel and Parikh[14]; a Rosenfeld two-body interaction was used. The third, designated "WIL," is a ground state computed by Wildenthal, using two-body matrix elements fitted to data over the entire $sd$ shell.[15] These matrix elements are not the same for all nuclei; rather they are given a mass dependence of $18/A^{1/3}$ to simulate the decrease of the matrix elements with increasing $A$. On occasion we will also use a fourth ground state, designated "PRO," which is a projected Hartree-Fock prolate $0^+$ solution.[14] The $sd$ shell occupancies for these ground states are tabulated in Table I. In all cases, in the uncorrelated ground states, orbitals below the $sd$ shell are assumed to be completely filled, and orbitals above the $sd$ shell, completely empty. In addition to the occupancies for each ground state, it is necessary to specify the two-particle densities

$$\langle\Phi_0|[(A^+_\alpha A^+_\beta)^{JT}\times(A_\gamma A_\delta)^{JT}]^{J=0}_{T=0}|\Phi_0\rangle ,$$

TABLE I. Fractional occupancies for *sd*-shell orbitals.

| Ground state | $1d_{5/2}$ | $1d_{3/2}$ | $2s_{1/2}$ |
|---|---|---|---|
| Kuo/shell model | 0.5593 | 0.3333 | 0.6558 |
| Oblate PHF | 0.8217 | 0.1850 | 0.1600 |
| Wildenthal | 0.7409 | 0.2049 | 0.3676 |
| Prolate PHF | 0.6200 | 0.2725 | 0.5900 |

where $\alpha$, $\beta$, $\gamma$, and $\delta$ are *sd* shell orbitals for each of the ground states; there are 63 of these numbers for *sd* shell nuclei. It should be noted that, for a Hamiltonian with one- and two-body parts, as we have employed, the OSRPA is sensitive to both the one-body densities (i.e., the occupancies) and the two-body densities of the ground state, but not to higher-order correlations.

The single-particle energies employed were obtained by the interpolation procedure of Ref. 16, and tabulated in Table II. The two-body residual interaction used is almost identical to the CAL interaction of Gillet and Sanderson[3]; the parameters are listed in the Appendix. Harmonic oscillator basis states are used throughout. Unless otherwise stated, an oscillator parameter

$$b=(\hbar/m\omega)^{1/2}=1.80 \text{ fm}$$

is used; this value is chosen to give the same charge rms radius as elastic electron scattering results.[17] Isospin is assumed to be a good quantum number, and neutrons and protons are not treated separately.

## IV. EXPERIMENTAL AND THEORETICAL RESULTS

In this section we show the measured electromagnetic form factors for the strongly excited negative-parity states of $^{28}$Si, and these are compared to open-shell RPA calculations. The form factors for the negative-parity $T=0$ states are presented first ($5^-$, $3_1^-$, $3_2^-$, etc.), followed by the negative-parity $T=1$ states ($6^-$, $5^-$, $4^-$). In open-shell nuclei, the shape of the Hartree-Fock field may change radically from that of the ground state. This change is not considered in the RPA excitation of the negative-parity states of $^{28}$Si from a shell-model ground state.

TABLE II. Single particle energies.

| Orbital | Energy |
|---|---|
| $1p_{3/2}$ | −3.9503 |
| $1p_{1/2}$ | 0.3814 |
| $1d_{5/2}$ | 7.1532 |
| $2s_{1/2}$ | 10.7028 |
| $1d_{3/2}$ | 13.2399 |
| $1f_{7/2}$ | 17.8425 |
| $2p_{3/2}$ | 19.3122 |
| $2p_{1/2}$ | 21.9932 |
| $1f_{5/2}$ | 25.7843 |

### A. The $5^-$ $T=0$ (9.702 MeV) state

The $5^-$ $T=0$ state is of interest because, in the context of the shell model, it is the simplest negative- and natural-parity state in $^{28}$Si. This state was previously studied via the $(p,\gamma)$ reaction by Lam *et al.*[18] This peak is obscure in electron scattering at $\theta=160°$, where transverse excitations dominate, but is very prominent at $\theta=90°$.

The experimental data are shown in Fig. 2, together with the OSRPA calculations. The total squared form factor is obviously predominantly Coulomb, in agreement with the OSRPA predictions. No renormalization is necessary to obtain the theoretical results for Fig. 2, but it is necessary to

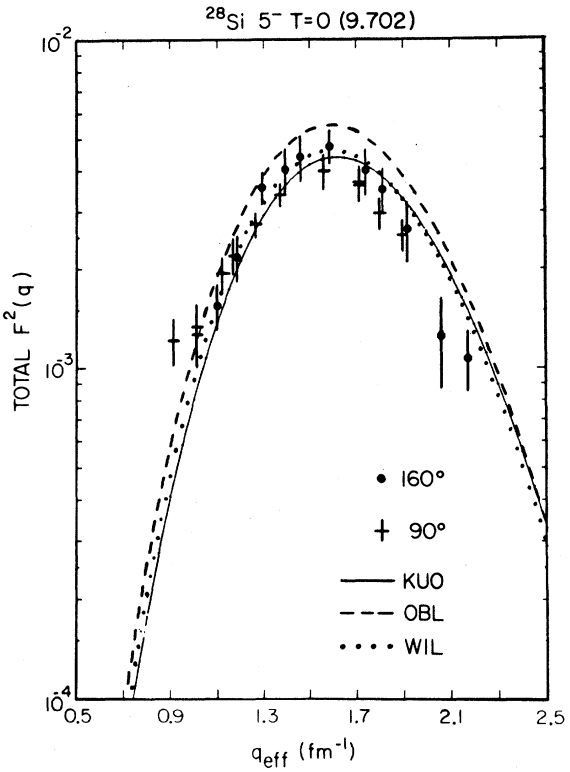


FIG. 2. Experimental total squared form factor for the $5^-$ $T=0$ (9.702 MeV) peak, for $\theta=160°$ (solid disks) and $\theta=90°$ (crosses). The solid, dashed, and dotted lines are the OSRPA predictions for the total squared form factor at $\theta=160°$ for the Kuo/shell model, oblate PHF, and Wildenthal ground states, respectively. In each case the lowest-energy $5^-$ $T=0$ OSRPA state is plotted. An oscillator parameter of $b=1.91$ fm was used to obtain the best fit to the data.

increase the oscillator parameter to a value of $b=1.91$ fm in order to achieve a reasonable fit to the data. Even with this adjustment the fit is not within experimental errors.

The experimental data show a small enhancement of $F^2(q)$ at $\theta=160°$ over that at $\theta=90°$, and this provides a measure of the small transverse squared form factor $F_T{}^2(q)$. Figure 3 shows the $F_T{}^2(q)$ extracted from the data, together with the OSRPA predictions. Although the error bars are large, and only upper limits can be established at some values of $q_{\text{eff}}$, the transverse data appear to favor the OSRPA prediction based on the Kuo/shell model ground state.

In this example it is seen that the Coulomb squared form factors have the same shape for the OSRPA $5^-$ states built on all three ground states, while the corresponding transverse squared form factors are of drastically differing shapes. Thus, $F_T{}^2(q)$, although small, is an important quantity to determine experimentally, since it is a sensitive measure of the parentages of the excited state. The differing parentage predicted by the various models considered are shown in Fig. 4. It is interesting that the $1f_{7/2}$-$1d_{3/2}{}^{-1}$ configuration is predicted to be important by the OSRPA, and yet this configuration cannot even contribute if one naively regards $^{28}$Si as a closed $1d_{5/2}$ subshell.

Figure 5 shows the distribution of $5^-$ $T=0$ strength for $^{28}$Si as observed experimentally, and as predicted by the OSRPA. The experimental $B(C5)$ value is obtained from a Tassie model fit to the data, with $c=2.580$, $t=2.140$ fm, and a $\chi^2$ of 0.157. The $B(C5)$ has been reduced by $\frac{1}{2}$ for graphical purposes, and the large value reflects the large transition radius needed to fit the data. The $5_2^-$ $T=0$ state at $E_x=12.024$ MeV is not observed experimen-

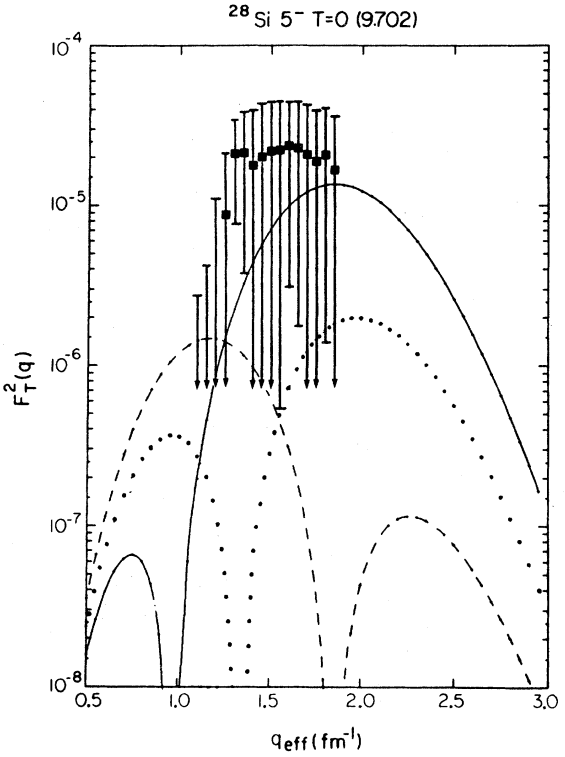


FIG. 3. Transverse squared form factor for the $5^-$ $T=0$ (9.702 MeV) state in $^{28}$Si. Solid squares are values of $F_T{}^2(q)$ extracted from the data of Fig. 2. Solid, dashed, and dotted lines show predictions for the lowest OSRPA $5^-$ $T=0$ states built on Kuo/shell model, oblate PHF, and Wildenthal ground states, respectively.

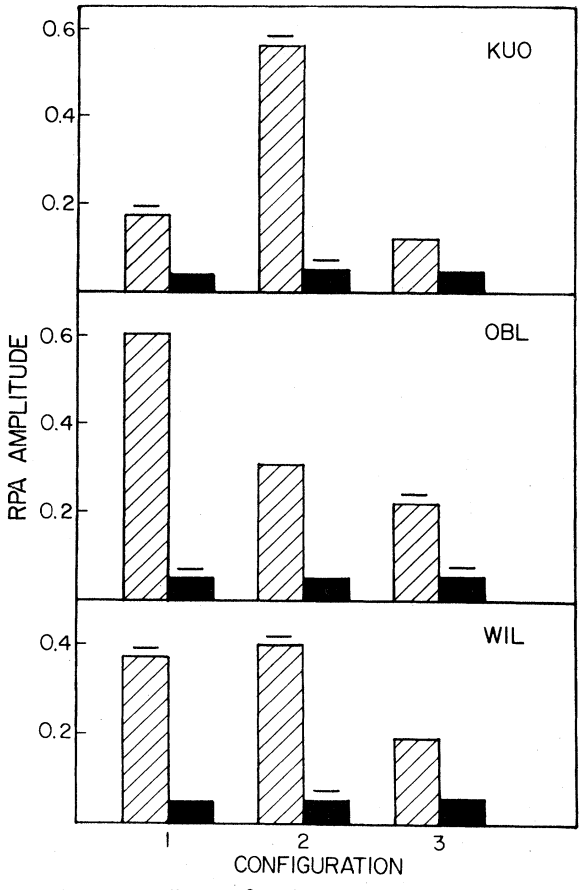


FIG. 4. Amplitudes for the lowest $5^-$ $T=0$ OSRPA state built on Kuo/shell model, oblate PHF, and Wildenthal ground states. The configuration numbers represent the following: $1=1f_{7/2}$-$1d_{5/2}{}^{-1}$, $2\equiv 1f_{7/2}$-$1d_{3/2}{}^{-1}$, $3\equiv 1f_{5/2}$-$1d_{5/2}{}^{-1}$. Forward amplitudes $F_{ph}$ are represented by hatched bars, backward amplitudes $F_{hp}$ by solid bars. The height of the bar represents the magnitude of $F_{ph}$ or $F_{hp}$. A minus sign over a bar denotes a negative amplitude.

tally, with an upper limit of $B(C5)<2\times10^{-5}$ $e^2$fm$^{10}$, assuming the same radial dependence as the $5_1^-$ $T=0$. It is apparent from Fig. 5 that the distribution of $5^-$ strength is quite sensitive to the ground state wave function used.

### B. The $3_1^-$ $T=0$ (6.879) MeV state

The first $3^-$ $T=0$ state in $^{28}$Si is located at $E_x=6.879$ MeV. There is a $4^+$ state only 10 keV away, at $E_x=6.889$ MeV,[19] and the experimental resolution is insufficient to resolve them. The squared form factor for this composite peak (Fig. 6) strongly suggests that more than one multipolarity is contributing. In Fig. 6 we also plot the $\theta=160°$ and $\theta=90°$ total squared form factors for the $4_2^+$ in $^{28}$Si, as predicted by the shell model calculations of Chung and Wildenthal.[20] To obtain these form factors from the wave functions of Chung and Wildenthal, effective charges of 0.5 for the neutron and 1.5 for the proton, and free nucleon $g$ factors, were assumed.

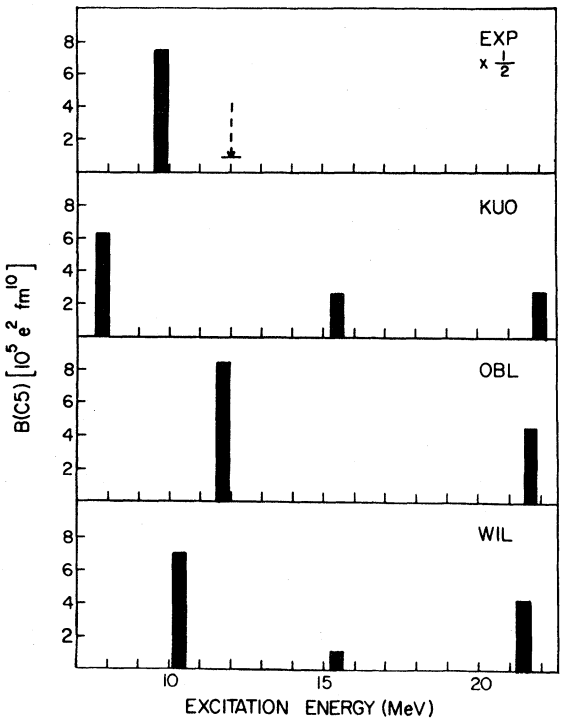


FIG. 5. Distribution of $5^-$ $T=0$ strength in $^{28}$Si, as observed experimentally, and as predicted by the OSRPA operating on the Kuo/shell model, oblate PHF, and Wildenthal ground states. The dashed arrow in the upper frame indicates the location and experimental upper limit for the strength of the unobserved $5_2^-$ $T=0$ state. Strengths shown in the upper frame have been multiplied by 0.5.

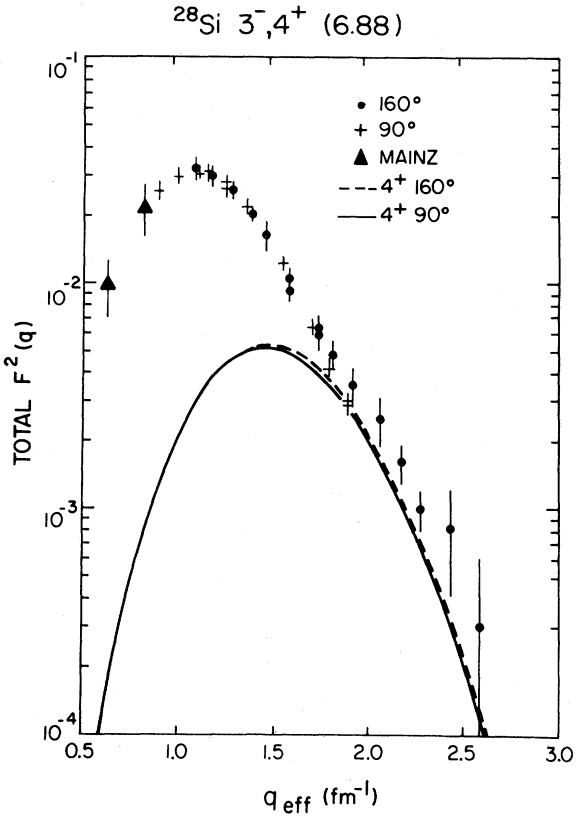


FIG. 6. Experimental total square form factor for the $3^-$ (6.879), $4^+$ (6.889) composite peak, for $\theta=160°$ and $\theta=90°$. The contribution of the $4^+$, as predicted by Chung and Wildenthal, and renormalized to fit the data, is shown by the dashed and solid lines. The $q_{\rm eff}=0.622$ fm$^{-1}$ and $q_{\rm eff}=0.847$ fm$^{-1}$ data points from Mainz were taken at $\theta=40°$ and $\theta=60°$, respectively.

The Chung-Wildenthal squared form factors are much larger than the experimental data points at the same $q$. To isolate the $3^-$ squared form factor, we assume that the $4^+$ theoretical squared form factor must be scaled down by a factor of 0.42 to give the true $4^+$ squared form factor. This scaling factor is chosen to make the $4^+$ squared form factor tangent to the data points at $q\approx1.9$ fm$^{-1}$, where the $3^-$ squared form factor is expected to reach a minimum.

In Fig. 7 are displayed the data points after the above-mentioned $4^+$ form factor is subtracted; this should be the form factor of the $3_1^-$ state alone. However, the result for $q_{\rm eff}>1.7$ fm$^{-1}$ is very sensitive to the precise size and shape of the $4^+$ form factor. Out to $q_{\rm eff}=1.7$ fm$^{-1}$, the $3_1^-$ squared form factor is pure Coulomb, within experimental error. At $q_{\rm eff}\approx1.12$ fm$^{-1}$, a Rosenbluth decomposition

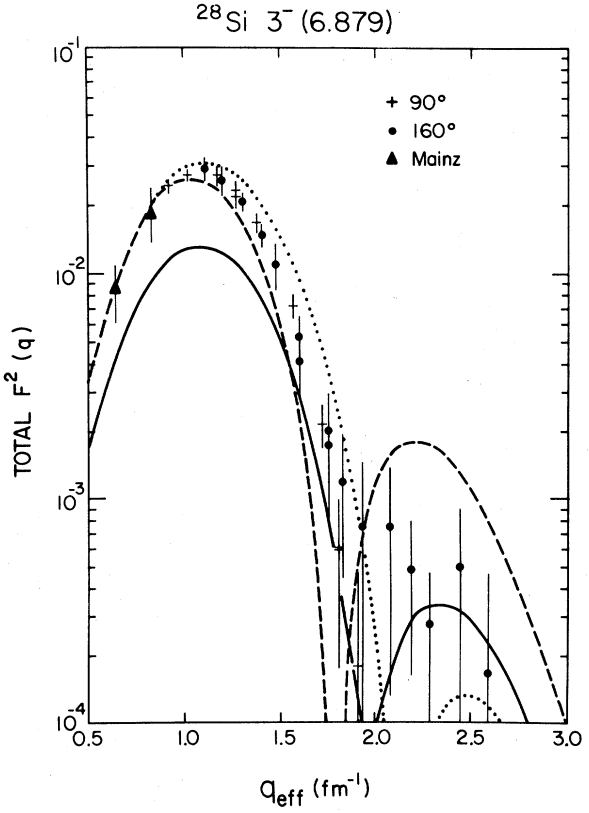


FIG. 7. The experimental points with the renormalized theoretical $4^+$ contribution subtracted. Solid, dashed, and dotted lines show predictions at $\theta=160°$ for the lowest OSRPA $3^-$ $T=0$ states built on Kuo/shell model, oblate PHF, and Wildenthal ground states, respectively. The two data points from Mainz have been renormalized by a factor of 0.9, and the renormalized contribution of the $4^+$ has been subtracted from them.

TABLE III. Configurations for the $3^-$ $T=0$ state in $^{28}$Si.

| Configuration number | Particle | Hole |
|---|---|---|
| 1 | $1d_{5/2}$ | $1p_{3/2}$ |
| 2 | $1d_{5/2}$ | $1p_{1/2}$ |
| 3 | $1d_{3/2}$ | $1p_{3/2}$ |
| 4 | $1f_{7/2}$ | $1d_{5/2}$ |
| 5 | $1f_{7/2}$ | $1d_{3/2}$ |
| 6 | $1f_{7/2}$ | $2s_{1/2}$ |
| 7 | $1f_{5/2}$ | $1d_{5/2}$ |
| 8 | $1f_{5/2}$ | $1d_{3/2}$ |
| 9 | $1f_{5/2}$ | $2s_{1/2}$ |
| 10 | $2p_{3/2}$ | $1d_{5/2}$ |
| 11 | $2p_{3/2}$ | $1d_{3/2}$ |
| 12 | $2p_{1/2}$ | $1d_{5/2}$ |

yields

$$F_c^2(q)=(2.77\pm0.17)\times10^{-2}$$

and

$$F_T^2(q)=(0.51\pm1.2)\times10^{-5}\,.$$

For $q>1.7$ fm$^{-1}$, the apparent nonzero $F_T^2(q)$, as manifested by an increase of $F^2$ ($\theta=160°$) over $F^2$ ($\theta=90°$), for $q_{\rm eff}>1.7$ fm$^{-1}$, is probably an artifact of incorrect subtraction of the $4^+$, since it is not known *a priori* how good the theoretical $4^+$ form factor is.

Also shown in Fig. 6 are two low-$q$ data points from the $(e,e')$ study of this state at Mainz.[21] The Mainz data cover $q_{\rm eff}$ from 0.6 to 2.0 fm$^{-1}$; the shape of their squared form factor agrees very well with ours, but the magnitude of our squared form factor is $\approx10\%$ smaller than that of the Mainz experiment.

Within the *p-ds-fp* model space considered, there are 12 possible particle-hole basis configurations which can give rise to $3^-$ states. These are tabulated in Table III. With both $lp\rightarrow sd$ and $sd\rightarrow fp$ excita-

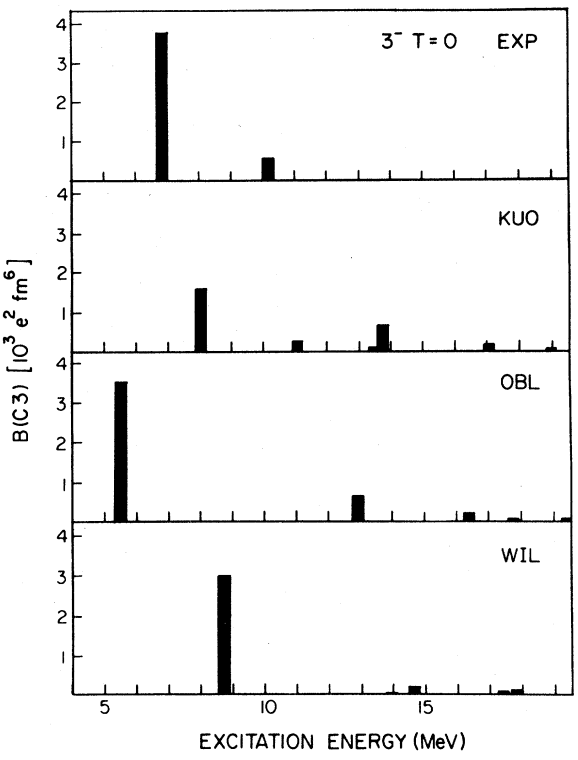


FIG. 8. Distribution of $3^-$ $T=0$ strength as observed experimentally, and as predicted by OSRPA operating on Kuo/shell model, oblate PHF, and Wildenthal ground states.

tions possible, the shape of the squared form factor will depend greatly on the actual admixture of basis states.

Figure 8 illustrates the distribution of $3^-$ $T=0$ strength calculated by the OSRPA for the three ground states of concern to us. In each case, a strong, low-lying $3^-$ $T=0$ state is predicted. Figure 7 shows the total squared form factors at $\theta=160°$ for the first OSRPA $3^-$ state in each case. The Kuo/shell model ground state predicts the correct shape for $F^2(q)$, but the magnitude is too small by a factor of 2.1. The oblate PHF ground state gives both the correct strength and approximately the correct shape. The Wildenthal ground state gives the correct strength but the predicted shape of $F^2(q)$ is too broad, indicating that the predicted parentage of this state is incorrect.

The parentages of the OSRPA $3_1^-$ states are illustrated in Fig. 9. The Kuo/shell model ground state yields a $3_1^-$ with predominantly $1f_{7/2}\rightarrow sd$ shell configurations, with small backward amplitudes, whereas the $3_1^-$ states built on the other two ground states are more heavily mixed in configuration and have larger backward amplitudes. All three ground states yield $3_1^-$ states with very small $F_T^2(q)$, in agreement with the data.

Table IV displays the Tassie model parameters and $B(C3)$ values for the $3_1^-$ and $3_2^-$ states of $^{28}$Si extracted from the experimental data.

### C. The $3_2^-$ $T=0$ (10.180 MeV) state

Experimentally, a second strong $3^-$ $T=0$ state is observed at $E_x=10.180$ MeV. As shown in Fig. 10, the experimental squared form factor is purely Coulomb. The Kuo/shell model ground state yields a second $3^-$ $T=0$ state at approximately the correct energy separation above the $3_1^-$ $T=0$ state (see Fig. 8), but of the wrong magnitude and also having a large $F_T^2(q)$, which is not observed experimentally. In fact, *all* the remaining $3^-$ $T=0$ OSRPA states built on the Kuo/shell model ground state display large $F_T^2(q)$, and hence cannot be identified with the 10.180 MeV state. The second $3^-$ built on the oblate PHF ground state is of approximately the correct strength and has a suitably small $F_T^2(q)$, but occurs too high in excitation energy, and is of the wrong shape, as shown in Fig. 10. Similarly, none of the higher $3^-$ OSRPA states built on the Wildenthal ground state has the correct shape and suitably small $F_T^2(q)$. The OSRPA, operating on all three ground states thus far considered, is unable to explain the 10.180 MeV $3^-$ $T=0$ state.

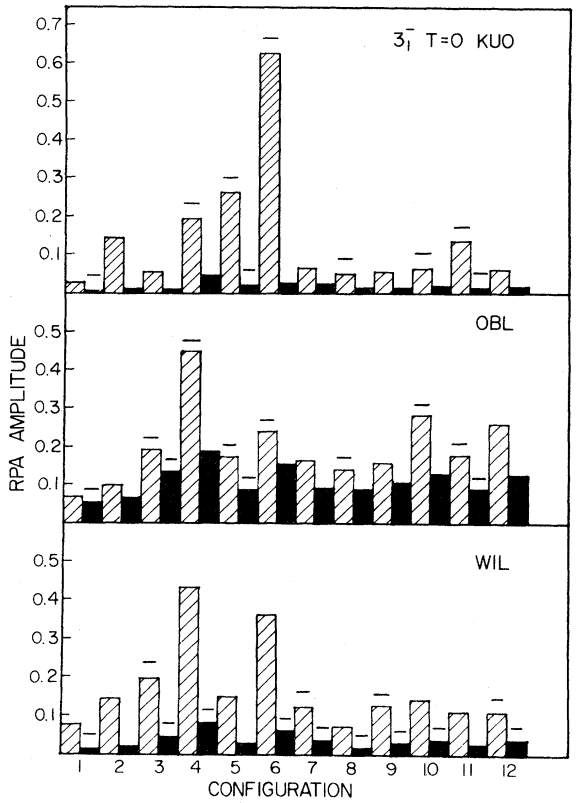


FIG. 9. Amplitudes for the lowest $3^-$ $T=0$ OSRPA states built on Kuo/shell model, oblate PHF, and Wildenthal ground states. Configurations 1–12 refer to configurations tabulated in Table III. Notation same as for Fig. 4.

Shown in Fig. 10 is the 160° total squared form factor for the *first* OSRPA $3^-$ state built on the *prolate* PHF ground state. The magnitude needs to be decreased by a factor of 4 to fit the data, but the shape is correct. In agreement with experiment, the OSRPA predicts $F_T^2(q)$ to be negligible. It is perhaps plausible that, since the $^{28}$Si PHF intrinsic state is relatively "soft" to deformation (the energy difference between oblate and prolate PHF solutions being only $\sim 1$ MeV out of a total binding energy of

TABLE IV. Tassie model fits to the $3^-$ $T=0$ states in $^{28}$Si.

| State | $c$ (fm) | $t$ (fm) | $B(C3\uparrow)$ ($e^2$fm$^6$) | $\chi^2$ |
|---|---|---|---|---|
| $3_1^-$ | 2.865±0.037 | 2.438±0.068 | (3.87±0.75)×10$^3$ | 0.65 |
| $3_2^-$ | 2.625±0.027 | 2.179±0.040 | (5.47±1.41)×10$^2$ | 0.14 |

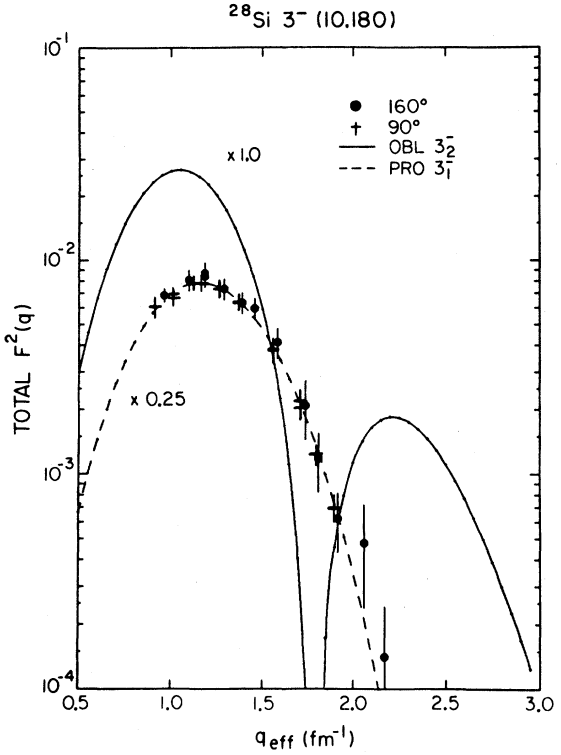


FIG. 10. $3_2^-$ $T=0$ (10.180 MeV) total squared form factor. Experimental points are shown by solid disks and crosses. The solid line is the second lowest OSRPA $3^-$ state built on the oblate PHF ground state. The dashed line is the lowest OSRPA $3^-$ state built on the prolate PHF ground state, reduced by factor 0.25 to fit the data. Theoretical curves are for $\theta=160°$.

$\sim$136 MeV),[14] the actual $^{28}$Si ground state may be a linear combination of oblate and prolate shapes, with the oblate component being predominant. Indeed, Bar-Touv and Goswami[22] have suggested, from other considerations, that the $0^+$ states of $^{28}$Si should be mixed in shape. The $3_1^-$ (6.879) state would then perhaps be a particle-hole excitation of the oblate component (with other smaller components mixed in to give the proper shape to the form factor), whereas the $3_2^-$ (10.180) state would be a particle-hole excitation of the prolate component. Alternatively, one could imagine the excitation of a particle-hole pair is coupled to deformation of the average field of the nucleus. The average field for $^{28}$Si in the $3_1^-$ excited state could be oblate in shape, which would strongly overlap with the large oblate component of the ground state wave function. Similarly, the average field of the $3_2^-$ state could be prolate in shape, which would overlap with the smaller prolate component of the ground state wave function. Figure 11 shows the RPA amplitudes for the

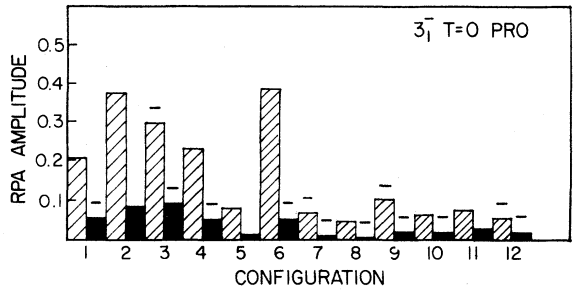


FIG. 11. RPA amplitudes for the lowest $3^-$ $T=0$ OSRPA state built on the prolate PHF ground state, before renormalization to fit the data. The notation is the same as for Fig. 4.

lowest $3^-$ state built on the prolate PHF ground state, *before* renormalizing to fit the data.

It is perhaps surprising that the Wildenthal ground state, which is derived from matrix elements fitted to experimental data, is not more successful than it is. The data used in the fitting are mostly from low-lying levels in the *ds* shell, with a strong bias towards those matrix elements which are important for the oblate configuration of $^{28}$Si. Hence a ground state which is the best fit to low-lying data may not be adequate to describe higher-energy excitations with a predominantly prolate configuration.

### D. The $1^-$ $T=0$ (8.904 MeV) state

The $1^-$ $T=0$ state at $E_x=8.904$ MeV was observed at both $\theta=90°$ and $\theta=160°$. The data are shown in Fig. 12. Figure 13 shows a Rosenbluth decomposition of the Coulomb and transverse squared form factors for this state.

In the model space of the *p-ds-fp* shells, there are 13 particle-hole configurations which can couple to $1^-$. This is similar to the number of configurations for the $3^-$ $T=0$ state, and one might expect similarly good fits. However, as Fig. 12 shows, the agreement between theory and experiment is much worse for the $1^-$ $T=0$ state. Moreover, the $1_1^-$ states built on the three different ground states differ greatly from each other in size and shape.

The likely source of difficulty is the mixing of the spurious center of mass motion with the calculated $1^-$ $T=0$ states. For a translationally invariant Hamiltonian, the RPA automatically separates out the spurious solution and assigns it zero excitation energy.[23] However, realistic shell model Hamiltonians, with an assumed fixed center of force, are not translationally invariant, with the result that spurious components may be mixed into the states of nonzero excitation energy.

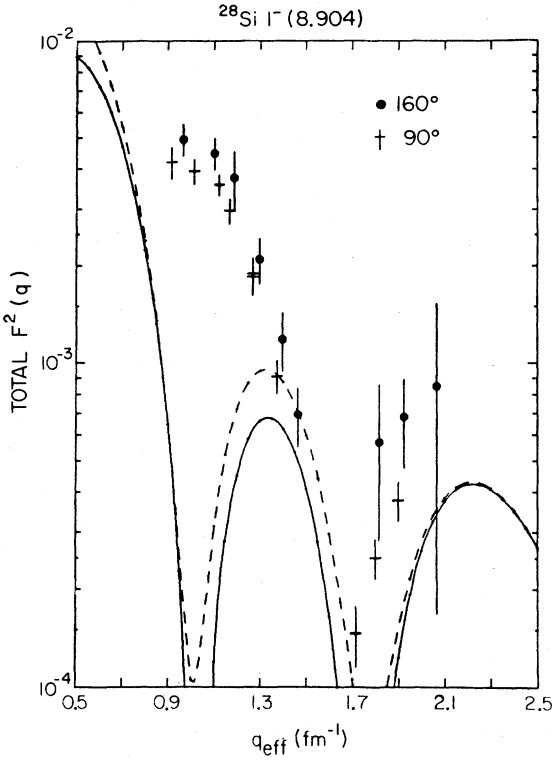


FIG. 12. $1^-$ $T=0$ (8.904) total squared form factor. Experimental points are shown by solid disks ($\theta=160°$) and crosses ($\theta=90°$). Dashed and solid lines are the predicted total squared form factor at $\theta=160°$ and $\theta=90°$, respectively, for the $1_1^-$ $T=0$ state built on the Wildenthal ground state. The disagreement between theory and experiment is even worse for the $1^-$ states built on the other ground states.

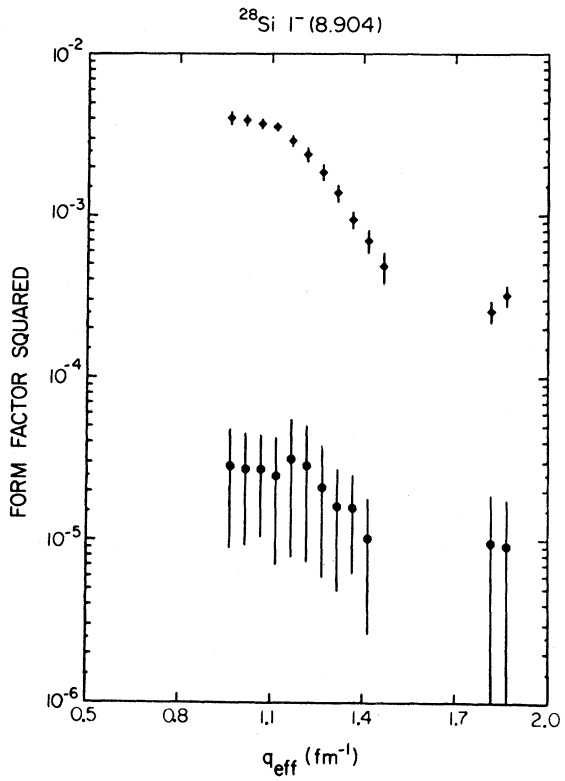


FIG. 13. Coulomb and transverse squared form factors for the $1^-$ $T=0$ (8.904 MeV) state in $^{28}$Si, extracted from the data of Fig. 12. The open diamonds denote $F_c^2(q)$ while the solid disks denote $F_t^2(q)$.

### E. The $1^-$, $2^-$, $T=0$ (9.929 MeV) state

The $E_x=9.929$ MeV state is listed in the compilation of Endt and Van der Leun[19] with an ambiguous spin assignment of $(1,2)^-$. This assignment was deduced on the basis of $l=1$ angular distributions in $^{27}$Al$(d,n)^{28}$Si and $^{29}$Si$(p,d)^{28}$Si reactions.[24,25] The experimental squared form factor for this state is shown in Fig. 14, and the Rosenbluth decomposition into $F_c^2(q)$ and $F_T^2(q)$ is shown in Fig. 15.

If this state were a pure $2^-$ excitation, the transition would be $M2$ and $F_c^2(q)$ would be zero. Since the data show both $F_c^2(q)$ and $F_T^2(q)$ to be nonzero, the state cannot be pure $2^-$. It can be either a pure $1^-$, or a composite of a $1^-$ and a $2^-$ state spaced very closely together.

### F. The $3^-$ $T=0/6^-$ $T=0$ (11.58 MeV) complex

The $6^-$ $T=0$ state, like the $6^-$ $T=1$, is expected to be dominated by the $1f_{7/2}$-$1d_{5/2}{}^{-1}$ particle-hole configuration. Being a "stretched" state, the $6^-$ can be excited in a one-step process only through the spin transition density. This makes possible a direct comparison between the cross sections observed in $(e,e')$ and $(p,p')$.[26] Because the spectroscopic factors in $(p,p')$ are smaller for the $6^-$ $T=0$ than for the $6^-$ $T=1$ states, in both $^{28}$Si and $^{24}$Mg, Petrovich and Love[27] have suggested that the $T=0$ states have significantly different wave functions from the corresponding $T=1$ states, with more complicated many-particle-many-hole structure in the $6^-$ $T=0$. Thus it would be interesting to measure the electromagnetic form factor of the $6^-$ $T=0$.

A peak is observed in the $(e,e')$ spectrum at $E_x=11.58\pm0.015$ MeV. Unfortunately, in this range, there are two known states in $^{28}$Si, the $6^-$ $T=0$ at 11.577 MeV, and a $3^-$ $T=0$ at 11.585 MeV.[19] The experimental resolution is insufficient to resolve these. The experimental data are shown in Fig. 16.

The $6^-$ $T=0$ is an $M6$ excitation, so its squared form factor should be purely transverse. A Rosenbluth decomposition of the data of Fig. 16 is shown.

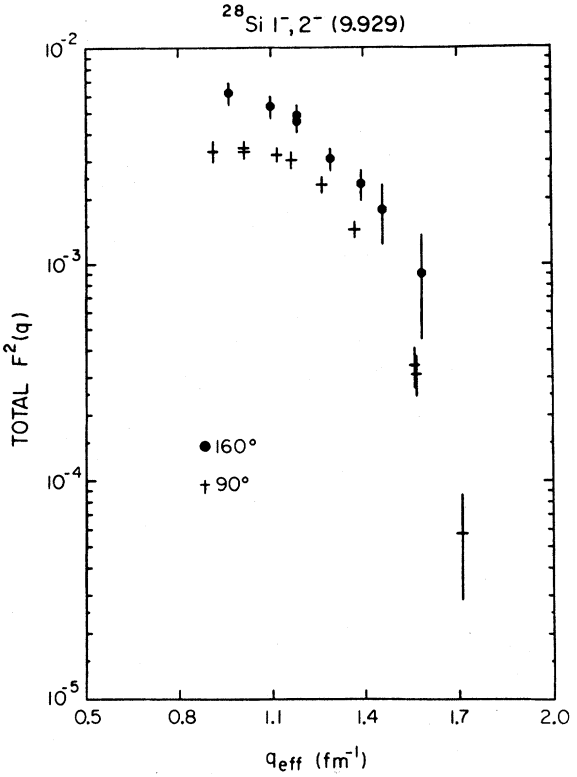


FIG. 14. Total squared form factor for the $1^-$, $2^-$ $T=0$ (9.929 MeV) state in $^{28}$Si. Experimental points are shown by solid disks ($\theta=160°$) and crosses ($\theta=90°$).

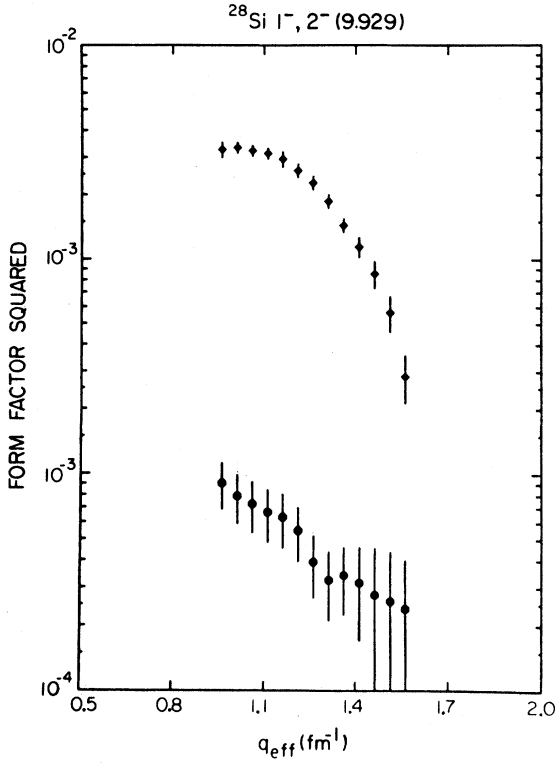


FIG. 15. Coulomb and transverse squared form factors for the $1^-$, $2^-$ $T=0$ (9.929 MeV) state, extracted from the data of Fig. 14. The open diamonds denote $F_c^2(q)$, while the solid disks denote $F_T^2(q)$.

in Fig. 17, together with the OSRPA predictions for the $6^-$ $T=0$. $F_c^2(q)$ can be attributed only to the $3^-$ $T=0$, whereas $F_T^2(q)$ can have contributions from both the $3^-$ $T=0$ and the $6^-$ $T=0$. Since $F_T^2(q)$ for the $3^-$ does not necessarily bear any relationship to $F_c^2(q)$ in either shape or size, it is not possible to extract the $6^-$ $T=0$ form factor. However, the local maximum in $F_T^2(q)$ near $q_{\text{eff}}\approx 1.8$ fm$^{-1}$ is perhaps indicative of a contribution from the $6^-$ $T=0$.

The salient features of the OSRPA calculations for the $6^-$ $T=0$ state in $^{28}$Si are contained in Table V.

It is noteworthy that a small amount of $T=1$ admixture would greatly enhance the strength of the squared form factor, since for spin excitations like the $6^-$ $T=1$ components are excited $\sim 28$ times more strongly than $T=0$ components. However, for the observed $F_T^2(q)$ to be entirely due to the $6^-$, a mixture is required:

$$|6^-\rangle = 0.98\,|6^-\ T=0\rangle + 0.19\,|6^-\ T=1\rangle\ ,$$

which seems like an improbably large amount of isospin mixing for two $6^-$ states separated in excitation energy by 2.8 MeV.

### G. The $6^-$ $T=1$ (14.356 MeV) state

The very prominent $6^-$ $T=1$ state was discussed in a previous paper.[28] We wish to present here the results of some recent calculations for the $6^-$ $T=1$, using the OSRPA.

As mentioned in Ref. 28, the observed $6^-$ strength is smaller than the theoretical strength as calculated in the OSRPA. We present in Table VI a summary of the calculations. The experimental $B(M6)$ value is obtained from the theoretical values simply by scaling down according to the ratio of $F^2(q)$ at the peak of the form factor. This is not strictly correct since the shape of the theoretical form factors does not match that of the experimental data.

It is seen that the theoretical $B(M6)$ depends strongly on the particular ground state used in the calculation. The factor by which the $M6$ strength is quenched thus ranges from 0.37 to 0.55, depending

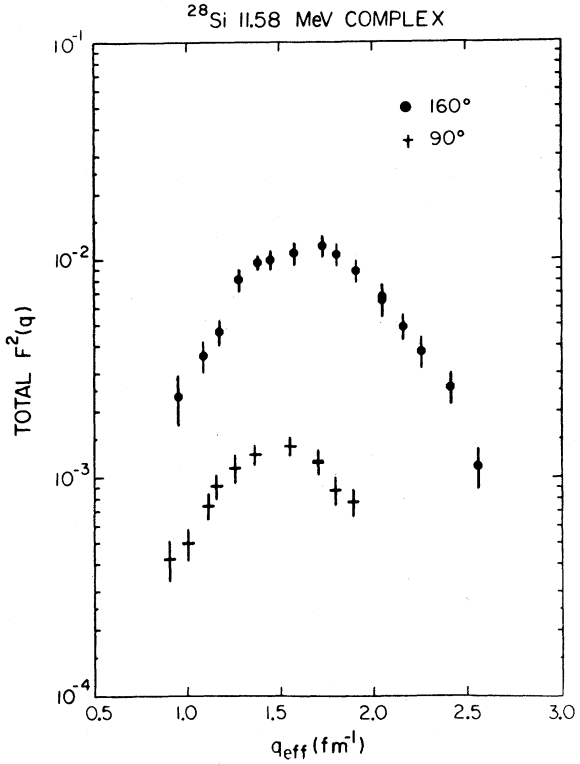


FIG. 16. The experimental total squared form factor for the 11.58 MeV complex. The solid disks denote data taken at $\theta=160°$; the crosses denote data taken at $\theta=90°$.

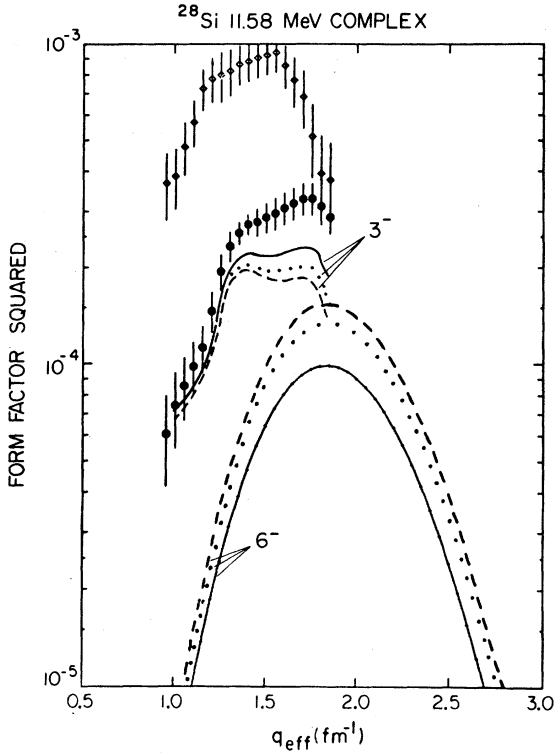


FIG. 17. Coulomb and transverse squared form factors for the data of Fig. 16. The open diamonds denote $F_c^2(q)$, while the solid disks denote $F_T^2(q)$. The solid, dashed, and dotted lines marked "6⁻" are the OSRPA predictions for the $6^-$ $T=0$ transverse squared form factor, for the Kuo/shell model, oblate PHF, and Wildenthal ground states, respectively. The lines marked "3⁻" are the remaining part of $F_T^2(q)$ after the corresponding $6^-$ contribution has been subtracted. An oscillator parameter of $b=1.8$ fm was used in the calculations.

on the model ground state. Thus, in any discussion of quenching of magnetic strength due to, e.g., renormalization of nucleon magnetic moments, it may be safest to restrict the discussion to closed-shell nuclei, since the ground states of open-shell nuclei are perhaps less well known.

### H. The $5^-$ $T=1$ (13.248 MeV) state

The $5^-$ $T=1$ state at $E_x=13.248$ MeV has been investigated via the $(p,\gamma)$ reaction by Lam *et al.*[18] There are several known states[19] in the vicinity of the $5^-$ within the energy resolution of this experiment, so the observed peak at $13.244\pm0.010$ MeV may actually be a composite of several unresolved peaks. In fact, the observed squared form factor does not resemble that of a $5^-$ state, so the $5^-$ contribution to the strength of the observed peak is probably small. However, we can use the strength of the peak to put an upper limit on the strength of the $5^-$ $T=1$. The experimental data are shown in Fig. 18.

The OSRPA calculations are summarized in Table VII. It is seen that if the $E_x=13.248$ MeV peak is identified with the OSRPA $5_1^-$ $T=1$ state,

TABLE V. OSRPA predictions for the $6^-$ $T=0$ state in $^{28}$Si, assuming a $1f_{7/2}$-$1d_{5/2}{}^{-1}$ configuration and $b=1.8$ fm.

| Ground state | $E_x$ (MeV) | $B(M6)$ ($\mu_N{}^2$fm$^{10}$) | $F_{ph}$ (fore) | $F_{hp}$ (back) |
|---|---|---|---|---|
| Kuo/shell model | 16.983 | $3.878\times10^7$ | 0.74804 | 0.01628 |
| Oblate PHF | 14.621 | $5.838\times10^7$ | 0.90652 | 0.00867 |
| Wildenthal | 15.382 | $5.134\times10^7$ | 0.86096 | 0.01889 |

TABLE VI. OSRPA predictions for the $6^-$ $T=1$ state in $^{28}$Si, assuming a $1f_{7/2}$-$1d_{5/2}{}^{-1}$ configuration and $b=1.8$ fm.

| Ground state | $E_x$ (MeV) | $B(M6)$ ($\mu_N{}^2$ fm$^{10}$) | $F_{ph}$ (fore) | $F_{hp}$ (back) |
|---|---|---|---|---|
| Kuo/shell model | 17.397 | $1.088\times10^9$ | 0.4320 | 0.0137 |
| Oblate PHF | 14.843 | $1.647\times10^9$ | 0.5234 | 0.0088 |
| Wildenthal | 15.655 | $1.462\times10^9$ | 0.4971 | 0.0122 |
| Experiment | 14.356 | $6.022\times10^8$ | | |

then the observed strength is much less than the predicted strength. The OSRPA predicts, and the data show, a large transverse component to $F^2(q)$; an analysis of the OSRPA amplitudes reveals that for $q>1$ fm$^{-1}$, $F_T{}^2(q)$ is dominated by the spin part of the transverse electric operator. However, reduction of the nucleon spin $g$ factor, sometimes suggested as the mechanism for the quenching of magnetic excitations,[29] cannot explain the observed lack of $5^-$ $T=1$ strength, since the OSRPA prediction for $F_c{}^2(q)$ alone exceeds the observed *total* squared form factor, and $F_c{}^2(q)$ does not depend on spin magnetic moments. It is implausible that the 13.248 MeV peak can be identified with the OSRPA $5_2^-$ or $5_3^-$ $T=1$ states, since no $5^-$ $T=1$ peak of the predicted strength is observed at lower excitation energies. A similar but less drastic, quenching is observed for the $5^-$ $T=1$ in $^{24}$Mg.[8]

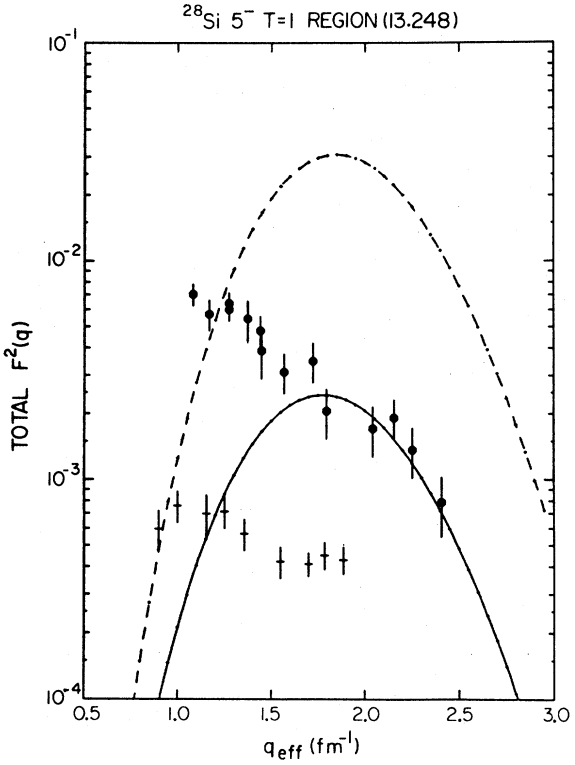


FIG. 18. Experimental total squared form factor for the 13.24 MeV peak, for $\theta=160°$ (solid disks) and $\theta=90°$ (crosses). The dashed and solid lines show the total squared form factor for $\theta=160°$ and $\theta=90°$, respectively, for the $5_1^-$ $T=1$ built on a Wildenthal ground state. The agreement between theory and experiment for the other ground states is even worse.

The apparent quenching may in fact be due to fragmentation of the $5^-$ $T=1$ strength due to coupling of the particle-hole OSRPA $5_1^-$ state with other degrees of freedom in the nucleus. The $5^-$ $T=1$ state at $E_x=13.248$ MeV may therefore be the lowest lying of these fragments, with other $5^-$ $T=1$ fragments yet to be discovered.

### I. The $4^-$ $T=1$ (12.664 MeV) state

A prominent peak is observed at $E_x=12.66\pm0.015$ MeV; this we tentatively identify with the $4^-$ $T=1$ state at $E_x=12.664$ MeV. Out to $q_{\text{eff}}=1.9$ fm$^{-1}$, which is the largest $q$ at which data were taken at both 160° and 190°, the squared form factor is almost purely transverse (see Fig. 19). This is what we expect for an $M4$ transition. In fact, at $q_{\text{eff}}\approx1.55$ fm$^{-1}$, a Rosenbluth decomposition gives

$$F_T{}^2(q)=(8.8\pm1.0)\times10^{-4}\,,$$

$$F_c{}^2(q)=(2.35\pm2.24)\times10^{-4}\,.$$

In the discussion of the $5^-$ $T=0$ state, we saw that states of different parentages could have the

TABLE VII. OSRPA predictions for the $5_1^-$ $T=1$ state. Column two is the height of the first maximum of $F_c{}^2(q)$. Column three is the height of the first maximum of the total squared form factor, as measured at a scattering angle of $\theta=90°$. The maxima are reached at values of $q_{\text{eff}}$ between 1.7 fm$^{-1}$ and 1.8 fm$^{-1}$ in each case.

| Ground state | Max $F_c{}^2(q)$ | Max $F^2(q)_{90}$ | $E_x$ |
|---|---|---|---|
| Kuo/shell model | $1.36\times10^{-3}$ | $3.23\times10^{-3}$ | 10.038 |
| Oblate PHF | $1.61\times10^{-3}$ | $1.73\times10^{-3}$ | 15.428 |
| Wildenthal | $1.13\times10^{-3}$ | $2.42\times10^{-3}$ | 14.293 |

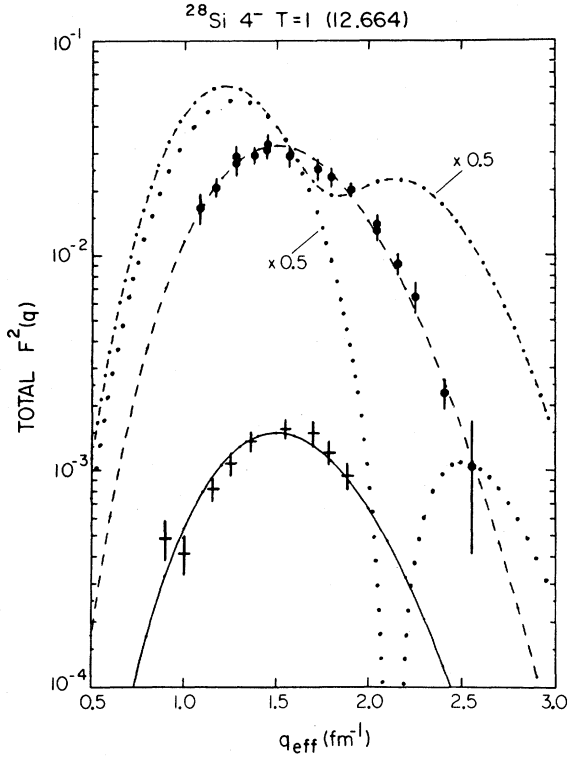


FIG. 19. Experimental total squared form factor for the $4^-$ $T=1$ (12.664 MeV) peak, for $\theta=160°$ (solid disks) and $\theta=90°$ (crosses). The dashed line and solid line are the $\theta=160°$ and $\theta=90°$ total squared form factors, respectively, for the contrived $1d_{5/2}$-$1p_{3/2}{}^{-1}$ configuration listed in Table VIII. The dotted line is the $4_1^-$ $T=1$ OSRPA state built on an oblate PHF ground state, reduced by a factor of 0.5. The dashed-dotted line is the sum of the squared form factors for the $4_1^-$ and $4_2^-$ $T=1$ states built on the oblate PHF ground state.

same shape for $F_c{}^2(q)$, but that measuring both $F_c{}^2(q)$ and $F_T{}^2(q)$ imposes more stringent constraints on the parentage. For magnetic states such as the $4^-$, $F_c{}^2(q)$ is always zero, so there is no "second constraint" and the parentage cannot be unambiguously deduced from the $(e,e')$ results alone. As an example, the three contrived sets of RPA amplitudes listed in Table VIII were all found to give good fits to the data (see Fig. 19). Because this is not a "stretched" state, both spin and orbital current densities can contribute to the transition, and these cannot be separately extracted from the data in a model-independent fashion. For the above three contrived configurations, it is found that configuration 2 is a pure spin-flip transition, whereas the other configurations have large orbital contributions as well. The excitation of this state by a different probe (e.g., protons) which has a *different* relative sensitivity to the spin and orbital densities, together with the $(e,e')$ data, would enable one to separate out the spin and orbital densities.

TABLE VIII. Contrived RPA amplitudes which fit the $4^-$ $T=1$ data. Note that set 3 has two particle-hole configurations.

| | Configuration | $F_{ph}$ (fore) | $F_{hp}$ (back) | $b$ (fm) |
|---|---|---|---|---|
| Set 1 | $1f_{5/2}$-$1d_{5/2}{}^{-1}$ | 0.6345 | 0.0 | 1.80 |
| Set 2 | $1d_{5/2}$-$1p_{3/2}{}^{-1}$ | 0.2436 | 0.0 | 1.80 |
| Set 3 | $1f_{7/2}$-$1d_{3/2}{}^{-1}$ | 0.3750 | 0.0 | 1.77 |
| | $1f_{5/2}$-$1d_{3/2}{}^{-1}$ | −0.1211 | 0.0 | |

The OSRPA is *totally unsuccessful* in explaining the observed squared form factor for this $4^-$ $T=1$ state. For all the ground states, the predicted $4_1^-$ $T=1$ state exhibits a much narrower squared form factor than is observed experimentally, indicating an unexpectedly small transition radius. The graph of $F^2$ (160°) for the oblate PHF ground state, shown in Fig. 19, is typical.

Calculations were also performed in which the nucleon spin magnetic moments were decreased by a factor of 0.75, but the RPA amplitudes were left unchanged. For a pure spin-flip transition, $F_T{}^2(q)$ would be decreased by $(0.75)^2\simeq 0.56$, approximately the quenching factor observed for the $6^-$ $T=1$ state. For the $4_1^-$ $T=1$ OSRPA states built on the three ground states of concern to us, this decrease in spin magnetic moments resulted in almost no change in shape, and a decrease in the magnitude of $F_T{}^2(q)$ by 0.50—0.60; thus quenching of the nucleon magnetic moment is *not* the cause of the broad form factor.

The situation is further confused by the fact that at $E_x=12.644$ MeV, only 20 keV away, there is another resonance which Meyer *et al.*[30] tentatively designate $4^-$, but which Endt and Van der Leun[19] list only as $3^-$—$5^-$. Its strong decays[19] to the $5^-$ $T=0$ ($E_x=9.072$) and $3^-$ $T=0$ ($E_x=6.879$) is suggestive of $4^-$ $T=1$. However, to the end of August 1982 (Refs. 19 and 31) no experiment had ever been done explicitly to measure the spin of the $E_x=12.644$ resonance via, e.g., angular correlations of decay $\gamma$ rays. If this resonance is $4^-$ $T=1$, then there are two $4^-$ $T=1$ states within 20 keV of one another, and the experimentally observed squared form factor is a composite of the squared form factors of the two states.

The calculations predict the $4_1^-$ and $4_2^-$ $T=1$ states to be fairly closely spaced (see Fig. 20). Unfortunately the sum of the $4_1^-$ and $4_2^-$ squared form factors, for any one of the four model ground states considered, does not resemble the observed squared form factor. The sum of $4_1^-$ and $4_2^-$ squared form

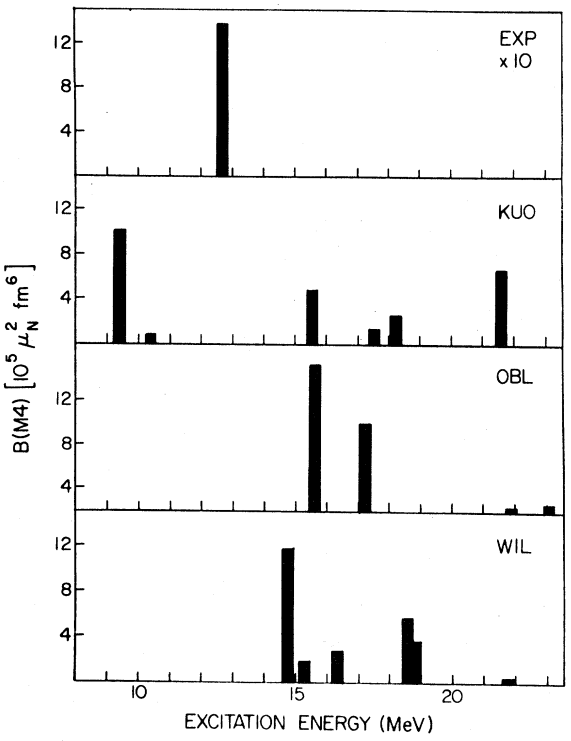


FIG. 20. Distribution of $4^-$ $T=1$ strength as observed experimentally, and as predicted by the OSRPA operating on the Kuo/shell model, oblate PHF, and Wildenthal ground states. The experimental value was obtained from the $B(M4)$ value of the contrived $1d_{5/2}$-$1p_{3/2}{}^{-1}$ configuration of Table VIII. Because the OSRPA predicts a larger transition radius than is observed, and since $B(M4)\sim r^6$, the predicted $B(M4)$'s are much larger than the experimental value, which has been multiplied by 10 for graphical purposes.

factors for the oblate PHF ground state, shown in Fig. 19, is the most favorable case; the analogous sum for the other ground states shows an even more marked dip at $q\approx 1.8$ fm$^{-1}$.

It might seem plausible that, if there are two $4^-$ $T=1$ states only 20 keV apart, some residual interaction might cause the OSRPA states to be mixed, i.e.,

$$|4_1\rangle'=\alpha|4_1\rangle+\beta|4_2\rangle\ ,$$

$$|4_2\rangle'=-\beta|4_1\rangle+\alpha|4_2\rangle\ ,$$

and the total squared form factor which we observe would be the sum of $F^2(q)$ for $|4_1\rangle'$ and $|4_2\rangle'$, rather than the sum of $|4_1\rangle$ and $|4_2\rangle$. It is easy to show that $F^2(q)$ would be the *same* in both cases, as follows. If $|\Phi_0\rangle$ is the $^{28}$Si ground state, and

$$|4_1\rangle=0_1^+|\Phi_0\rangle \text{ and } |4_2\rangle=0_2^+|\Phi_0\rangle\ ,$$

then it follows that

$$|4_1\rangle'=P_1^+|\Phi_0\rangle \text{ and } |4_2\rangle'=P_2^+|\Phi_0\rangle\ ,$$

where

$$P_1^+=\alpha 0_1^+ +\beta 0_2^+\ ,$$

$$P_2^+=-\beta 0_2^+ +\alpha 0_1^+\ .$$

The summed squared form factor for the two unmixed states is, apart from a numerical factor, given by

$$F^2(q)=|\langle\Phi_0|M0_1^+|\Phi_0\rangle^2+|\langle\Phi_0|M0_2^+|\Phi_0\rangle|^2\ ,$$

while the summed form factor squared for the two mixed states is

$$F^2(q)'=|\langle\Phi_0|MP_1^+|\Phi_0\rangle|^2 + |\langle\Phi_0|MP_2^+|\Phi_0\rangle|^2\ ,$$

where $M$ is an electromagnetic operator.

Substituting for $P_1^+$ and $P_2^+$, and using the fact that $\alpha$ and $\beta$ are real numbers such that $\alpha^2+\beta^2=1$, it follows that $F^2(q)=F^2(q)'$. Thus, mixing has no effect on the summed squared form factor, and cannot explain the observed $F^2(q)$.

In conclusion, the OSRPA is unable to predict the observed, anomalously broad form factor. It would be desirable to establish the spin of the $E_x=12.644$ MeV resonance, since if it were a strong resonance in $(e,e')$ and *not* $4^-$ $T=1$, our previous analysis would be erroneous. It would also be desirable to redo this $(e,e')$ experiment with a thinner target to obtain high resolution, so that any interfering peak 20 keV away could be resolved.

## V. DISCUSSION

As a tool for predicting the properties of the negative-parity states of $^{28}$Si, the OSRPA is seen to be very sensitive to the ground state wave function used. In each case, a change in the ground state from Kuo/shell model to oblate PHF to prolate PHF to Wildenthal is observed to drastically change both the distribution of strength as a function of excitation energy, and the particle-hole configuration amplitudes of the individual states. In the OSRPA, the double-commutator formalism was specifically designed to make the OSRPA insensitive to many-body correlations of rank greater than two[4]; nonetheless, the calculations presented in this paper demonstrate that the results are *very* sensitive to one- and two-body densities of the ground state wave function. Of course, the uncertainty in the ground state must be resolved before the validity of the OSRPA itself can be tested against experimental data.

Other parameters which enter the calculations are the single-particle energies and the residual interaction. Variations in these quantities will also affect the results. The Gillet CAL interaction was obtained empirically by selecting calibration states in closed-shell nuclei whose structures were assumed to be adequately described by the RPA, and then varying the parameters of the interaction until the RPA predictions agreed with experiment. This interaction, obtained for closed-shell nuclei, is then assumed to be valid in open-shell nuclei. This is perhaps questionable. The Gillet interaction is density-independent, whereas the true nucleon-nucleon interaction depends on the local density of nuclear matter. The average density may not be the same in open-shell nuclei as in closed-shell nuclei, and so a residual interaction derived for closed shells may not be applicable in open shells.

The OSRPA assumes that the excited state is obtained from the ground state by promoting a single nucleon to a different orbital; all other nucleons are assumed to remain frozen in place. There is no provision for the possible rearrangement of the remaining core nucleons. But if the excited state is strongly collective, one might expect that excitation of one nucleon to be coupled to changes in the configuration of many of the remaining nucleons. Since such rearrangements of the core may have unknowingly occurred in the calibration states used to fit the parameters of the residual interaction, the interaction may already be partially renormalized for such core rearrangements. Of course, there is no *a priori* reason to believe that the core rearrangement associated with a calibration state should resemble that associated with another excited state in a different nucleus.

The $^{28}$Si nucleus is interesting in that it is soft to shape deformations, in contrast to the $^{24}$Mg nucleus, which is rigidly prolate. The electron scattering data for the $3_1^-$ and $3_2^-$ $T=0$ states in $^{24}$Mg and $^{28}$Si are very suggestive of this. In $^{24}$Mg, the OSRPA operating on a single shell model ground state is sufficient to reproduce the shapes of both $3_1^-$ and $3_2^-$ states,[8] whereas in $^{28}$Si, the $3_1^-$ resembles the OSRPA excitation of an oblate PHF ground state, while the $3_2^-$ resembles the OSRPA excitation of a prolate PHF ground state.

The coupling of a one-particle-one-hole configuration to other degrees of freedom in the nucleus, such as core rearrangement, can lead to fragmentation of the particle-hole strength. This was proposed as a possible explanation for the anomalously weak excitation of the $5^-$ $T=1$ state. The softness of the $^{28}$Si nucleus to shape deformations makes it especially vulnerable to such core rearrangement effects. Generally, when the observed strength of a single peak is less than predicted by theory, it is questionable whether the quenching is due to fragmentation of the strength or due to more exotic effects, such as meson exchange currents of $\Delta$-hole effects.

States such as the $6^-$ $T=1$ and the $5^-$ $T=0$ have only one or a very small number of contributing particle-hole configurations, and thereby offer the hope that the particle-hole structure may be sufficiently well understood that deviations between theory and experiment may be attributed to one or more of the complicated or exotic effects mentioned above. Such deviations do indeed exist. The quenching of the strength of the $6^-$ $T=1$ (Ref. 28) is part of a general pattern of quenching of magnetic strength in many different nuclei,[29] and has been attributed to renormalization of the nucleon magnetic moment,[29] to $\Delta$-hole effects,[32] and to many particle-many hole components in the wave function.[33] The OSRPA predicts the correct strength for the $5^-$ $T=0$, but an anomalously large oscillator parameter is required to achieve a satisfactory fit to the data. Discrepancies between theory and experiment for such simple states as the $6^-$ and the $5^-$ are a clear indication that there is much more new and interesting physics yet to be unraveled by the study of these states.

## VI. SUMMARY

The high resolution of the present experiment has enabled us to isolate, for the first time, the electromagnetic form factors of the $1^-$ $T=0$ (8.904), $5^-$ $T=0$ (9.702), $1^-$, $2^-$ $T=0$ (9.929), $3_2^-$ $T=0$ (10.180), and $4^-$ $T=1$ (12.664) states. The $3_1^-$ $T=0$ (6.879) state has been studied by subtracting off the theoretical contribution of the nearby $4^+$ (6.889) state. An upper limit for the squared form factor of the $5^-$ $T=1$ (13.248) has been established. The $3^-$ $T=0/6^-$ $T=0$ complex at 11.58 MeV remains unresolved.

The OSRPA predictions for these negative-parity states has been shown to be sensitive to the ground state wave function used. The Kuo shell model ground state is most successful for the $5^-$ $T=0$ state, the oblate PHF and Wildenthal ground states are most successful for the $3_1^-$ $T=0$ state, and the prolate PHF ground state is most successful for the $3_2^-$ $T=0$ state. None of the ground states used can reproduce the form factor of the $4^-$ $T=1$ state. The $5^-$ $T=1$ to be anomalously weak, leading to speculation that the strength may be fragmented. The small transverse squared form factor of the natural parity states is shown to be a sensitive measure of the parentage of the state.

## ACKNOWLEDGMENTS

The authors wish to thank Dr. S. S. M. Wong and Dr. D. J. Rowe of the University of Toronto for providing the OSRPA programs used in this investigation, and for many enlightening discussions. We wish to express our thanks also to Dr. B. H. Wildenthal of Michigan State University for providing his densities for the $^{28}$Si ground state. This research was supported by the Natural Sciences and Engineering Research Council, Canada, and by the U. S. Department of Energy under Contract Ey-76-C-02-3069.

## APPENDIX: GILLET FORCE PARAMETERS

The parameters are defined in terms of the singlet and triplet projection operators for spin and isospin $P_s(\sigma)$, $P_t(\sigma)$, $P_s(\tau)$, and $P_t(\tau)$, where

$$P_s(\sigma)=\tfrac{1}{4}(1-\vec{\sigma}_1\cdot\vec{\sigma}_2)\ ,$$

$$P_t(\sigma)=\tfrac{1}{4}(3+\vec{\sigma}_1\cdot\vec{\sigma}_2)$$

and analogously for $P_s(\tau)$ and $P_t(\tau)$. The two-body interaction is

$$V(r)=\exp[-(r/\mu)^2][C^{11}P_s(\tau)P_s(\sigma)+C^{13}P_s(\tau)P_t(\sigma)+C^{31}P_t(\tau)P_s(\sigma)+C^{33}P_t(\tau)P_t(\sigma)]\ ,$$

where

$$C^{11}=29.25\ \text{MeV}\ ,\quad C^{13}=-45.0\ \text{MeV}\ ,$$

$$C^{31}=-22.5\ \text{MeV},\quad C^{33}=6.75\ \text{MeV}\ ,$$

and

$$\mu=1.6795\ \text{fm}\ .$$

[1]D. H. Wilkinson, Physica (The Hague) 22, 1039 (1956).
[2]J. P. Elliott and B. H. Flowers, Proc. R. Soc. London A242, 57 (1957).
[3]V. Gillet and N. Vinh Mau, Nucl. Phys. 54, 321 (1964); V. Gillet and E. A. Sanderson, *ibid.* 54, 472 (1964); V. Gillet and M. A. Melkanoff, Phys. Rev. 133, B1190 (1964); V. Gillet, A. M. Green, and E. A. Sanderson, Nucl. Phys. 88, 321 (1966).
[4]D. J. Rowe, Rev. Mod. Phys. 40, 153 (1968); Nucl. Phys. A107, 99 (1968); *Nuclear Collective Motion* (Methuen, London, 1970), Chaps. 13 and 14; in *Dynamic Structure of Nuclear States,* edited by D. J. Rowe, L. E. H. Trainor, S. S. M. Wong, and T. W. Donnelly (University of Toronto Press, Toronto, 1972), p. 101; D. J. Row, S. S. M. Wong, H. Chow, and J. B. McGrory, Nucl. Phys. A298, 31 (1978).
[5]D. J. Rowe and S. S. M. Wong, Nucl. Phys. A153, 561 (1970).
[6]J. P. Blaizot and D. Gogny, Nucl. Phys. A284, 429 (1977); J. P. Blaizot, D. Gogny, and B. Grammaticos, *ibid.* A265, 315 (1976); J. P. Blaizot, Phys. Rep. 64, 173 (1980).
[7]J. P. Blaizot and L. Sips, Nucl. Phys. A337, 157 (1980); D. Goutte, J. B. Bellicard, J. M. Cavedon, B. Frois, M. Huet, P. Leconte, Phan Xuan Ho, S. Platchkov, J. Heisenberg, J. Lichtenstadt, C. N. Papanicolas, and I. Sick, Phys. Rev. Lett. 45, 1618 (1980).
[8]H. Zarek, S. Yen, R. J. Sobie, B. O. Pich, T. E. Drake, C. F. Williamson, S. Kowalski, and C. P. Sargent, Phys. Rev. C (to be published).
[9]W. Bertozzi, M. V. Hynes, C. P. Sargent, C. Creswell, P. C. Dunn, A. Hirsch, M. Leitch, B. Norum, F. N. Rad and T. Sasanuma, Nucl. Instrum. Methods 141, 457 (1977); W. Bertozzi, M. V. Hynes, C. P. Sargent, W. Turchinetz, and C. Williamson, *ibid.* 162, 211 (1979).
[10]T. de Forest, Jr. and J. D. Walecka, Adv. Phys. 15, 1 (1966).
[11]L. J. Tassie, Aust. J. Phys. 9, 407 (1956).
[12]J B. French, E. C. Halbert, J. B. McGrory, and S. S. M. Wong, in *Advances in Nuclear Physics,* edited by M. Baranger and E. Vogt (Plenum, New York, 1969), Vol. 3.
[13]T. T. S. Kuo, Nucl. Phys. A103, 71 (1967).
[14]B. Castel and J. C. Parikh, Phys. Rev. C 1, 990 (1970).
[15]B. H. Wildenthal, private communication. This new interaction supersedes the older Chung-Wildenthal interaction.
[16]S. S. M. Wong, D. J. Rowe, and J. C. Parikh, Phys. Lett. 48B, 403 (1974).
[17]G. C. Li, M. R. Yearian, and I. Sick, Phys. Rev. C 9, 1861 (1974); T. W. Donnelly and G. E. Walker, Ann. Phys. (N.Y.) 60, 209 (1970).
[18]S. T. Lam, A. E. Litherland, and R. E. Azuma, Can. J. Phys. 49, 685 (1971); G. F. Neal and S. T. Lam, Phys. Lett. 45B, 127 (1973).
[19]P. M. Endt and C. Van der Leun, Nucl. Phys. A310, 226 (1978).
[20]B. A. Brown, W. Chung, and B. H. Wildenthal, Phys. Rev. C 21, 2600 (1980).
[21]G. Mülhaupt Ph.D. thesis, Johannes Gutenberg University, 1970 (unpublished).
[22]J. Bar-Touv and A. Goswami, Phys. Lett. 28B, 391 (1969).
[23]D. J. Rowe, *Nuclear Collective Motion* (Methuen, London, 1970), Chaps. 13 and 14; D. J. Thouless, Nucl. Phys. 22, 78 (1961).
[24]W. Bohne, H. Fuchs, K. Grabisch, M. Hagen, H. Homeyer, U. Janetzki, H. Lettau, K. H. Maier, H. Morgenstern, P. Pietrzyk, G. Roschert, and J. A. Scheer, Nucl. Phys. A131, 273 (1969).

[25]G. J. Wagner, Nucl. Phys. A176, 47 (1971).
[26]R. A. Lindgren, W. J. Gerace, A. D. Bacher, W. G. Love, and F. Petrovich, Phys. Rev. Lett. 42, 1524 (1979).
[27]F. Petrovich, W. G. Love, A. Picklesimer, G. E. Walker, and E. R. Siciliano, Phys. Lett. 95B, 166 (1980).
[28]S. Yen, R. Sobie, H. Zarek, B. O. Pich, T. E. Drake, C. F. Williamson, S. Kowalski, and C. P. Sargent, Phys. Lett. 93B, 250 (1980).
[29]A. Richter, Nucl. Phys. A374, 193 (1982).
[30]M. A. Meyer, I. Venter, and D. Reitmann, Nucl. Phys. A250, 235 (1975).
[31]Phys. Abstr. January 1978 to August 1982.
[32]W. Weiss, Nucl. Phys. A374, 505 (1982); H. Arenhovel, *ibid.* A374, 521 (1982); J. Delorme, *ibid.* A374, 541 (1982).
[33]Dean Halderson, K. W. Kemper, J. D. Fox, R. O. Nelson, E. G. Bilpuch, C. R. Westerfeldt, and G. E. Mitchell, Phys. Rev. C 24, 786 (1981).